SPACE SCIENCES LABORATORY

DYNAMICAL THEORY OF LOW ENERGY ELECTRON DIFFRACTION

Final Report on: NASA Grant NGR 05-003-275

Principal Investigator:
Professor Harold P. Smith, Jr.

Space Sciences Laboratory Series 10, Issue 30

UNIVERSITY OF CALIFORNIA, BERKELEY

Space Sciences Laboratory
University of California
Berkeley, California 94720

DYNAMICAL THEORY OF LOW ENERGY ELECTRON DIFFRACTION

Final Report on

NASA Grant
NGR 05-003-275

Principal Investigator: Professor Harold P. Smith, Jr.

Space Sciences Laboratory Series 10, Issue 30

Abstract

An extended version of the Bethe theory of low energy electron diffraction (LEED) is presented and successfully applied to a computation of diffracted beam intensity as a function of wavelength of the incident electron. The results show consistent behavior with respect to parameter variation and are in reasonable agreement with measured beam intensities.

I. INTRODUCTION

The theory of Low Energy Electron Diffraction (LEED) has been the object of a number of recent investigations.[1—5] Most of these stress the importance of dynamical effects and point out the inadequacy of simple kinematic theory to describe accurately the dependence of the diffracted beam intensities on electron energy. The dynamical theories of LEED that have been proposed so far may be divided into two broad categories: (1) self-consistent field methods,[1] and (2) "matching" formalisms.[2—5] Our method, which is an extension of the Bethe theory,[6] belongs to the latter group. It assumes that the incident and the diffracted electron beams are plane waves and that the crystal can be represented by a three-dimensional, semi-infinite, periodic potential, cut off abruptly at a plane surface. The present paper consists of three parts: first, a brief review of the theory; then, a discussion of results of beam intensity calculations for a fcc lattice; and finally, a comparison with recent experimental results.[7]

II. THEORY

Consider a perfect crystal, represented by a complex, periodic potential, $W(\vec{r})$,

$$\left.\begin{aligned} W(\vec{r}) &= \sum_{\ell,m,n} w_{\ell,m,n}\, e^{2\pi i \vec{b}_{\ell,m,n} \cdot \vec{r}} && z < 0 \\ W(\vec{r}) &= 0 && z \geq 0 \end{aligned}\right\} \qquad (1)$$

where $\vec{b}_{\ell,m,n}$ is the reciprocal lattice vector. The wave function, $\psi(\vec{r})$, inside the crystal (i.e., for $z < 0$) may be written in the form

$$\psi(\vec{r}) = \int \sum_{\ell,m,n} \psi_{\ell,m,n}(\vec{p})\, e^{i\left[\vec{p} + 2\pi\vec{b}_{\ell,m,n}\right] \cdot \vec{r}}\, d\vec{p} \qquad (2)$$

where the integral extends over the first Brillouin zone, and $\psi_{\ell,m,n}$ is a function of the vector $\vec{p}$. In the case of a single incident electron beam, represented by a plane wave, the Bloch theorem may be invoked for the two surface dimensions (x and y). Thus, equation (2) becomes

$$\psi(\vec{r}) = \int \sum_{\ell,m,n} \psi_{\ell,m,n}(q)\, e^{i\left[\vec{p}(q) + 2\pi\vec{b}_{\ell,m,n}\right] \cdot \vec{r}}\, dq \qquad (3)$$

where the projection of $\vec{p}$ onto the surface normal is a function of the scalar quantity, q. However, the components of $\vec{p}$ parallel to the surface are independent of q. The integral in equation (3) may be

approximated by a sum,

$$\psi(\vec{r}) = \sum_{\ell,m,n,q} \psi_{\ell,m,n,q} \, e^{i\left(\vec{p}_q + 2\pi\vec{b}_{\ell,m,n}\right) \cdot \vec{r}} \tag{4}$$

and, finally, a vector $\vec{k}_{\ell,m,n,q} = \vec{p}_q + 2\pi\vec{b}_{\ell,m,n}$ may be defined such that

$$\psi(\vec{r}) = \sum_{\ell,m,n,q} \psi_{\ell,m,n,q} \, e^{i\vec{k}_{\ell,m,n,q} \cdot \vec{r}} \tag{5}$$

Equation (5) is a solution of the Schrodinger equation, $\nabla^2\psi(\vec{r}) + \left(K^2 + W(\vec{r})\right)\psi(\vec{r}) = 0$, if the coefficients $\psi_{\ell,m,n,q}$ satisfy the compatibility relations,

$$\psi_{\ell,m,n,q}\left(K^2 - k^2_{\ell,m,n,q}\right) + \sum_{\ell',m',n'} W_{\ell',m',n'}\psi_{\ell-\ell',m-m',n-n',q} = 0 \tag{6}$$

or in matrix form,

$$K^2\underset{\sim}{\psi} + A\underset{\sim}{\psi} = 0 \tag{7}$$

where $\underset{\sim}{\psi}$ is a vector whose components are the coefficients $\psi_{\ell,m,n,q}$, and A is a square matrix. Assuming that both the incident and the diffracted electron beams are plane waves, the wave function in the vacuum may be written as

$$\Phi(\vec{r}) = \sum_{\ell,m,n} \Phi_{\ell,m,n} \, e^{i\vec{h}_{\ell,m,n} \cdot \vec{r}} \qquad z \geq 0 \tag{8}$$

where

$$\left|\vec{h}_{\ell,m,n}\right| = K \tag{9}$$

The continuity of the wave function and its derivative with respect to the surface normal (z-direction), at the surface, z = 0, may be stated as

$$\sum_{\ell,m,n,q} \psi_{\ell,m,n,q} \, e^{i\vec{k}_{\ell,m,n,q} \cdot \vec{r}} = \sum_{\ell,m,n} \Phi_{\ell,m,n} \, e^{i\vec{h}_{\ell,m,n} \cdot \vec{r}} \tag{10}$$

$$\sum_{\ell,m,n,q} \psi_{\ell,m,n,q} \left(\vec{k}_{\ell,m,n,q} \cdot \vec{l}_z\right) e^{i\vec{k}_{\ell,m,n,q} \cdot \vec{r}} = \tag{11}$$

$$= \sum_{\ell,m,n} \Phi_{\ell,m,n} \left(\vec{h}_{\ell,m,n} \cdot \vec{l}_z\right) e^{i\vec{h}_{\ell,m,n} \cdot \vec{r}}$$

where $\vec{1}_z$ is a unit vector in the z-direction. Equations (10) and (11) must be satisfied for all values of x and y, and, therefore,

$$\left.\begin{aligned} \vec{k}_{\ell,m,n,q} \cdot \vec{1}_x &= \vec{h}_{\ell,m,n} \cdot \vec{1}_x \\ \vec{k}_{\ell,m,n,q} \cdot \vec{1}_y &= \vec{h}_{\ell,m,n} \cdot \vec{1}_y \end{aligned}\right\} \tag{12}$$

At this point, it is convenient to consider a specific case, e.g., a cubic lattice, in order to simplify the equations. This can be done without loss of generality, since the extension of the treatment to other lattices is straightforward. For a cubic lattice, with constant a, we have,

$$\vec{b}_{\ell,m,n} = \frac{1}{a}\,(\ell,m,n) \tag{13}$$

Combining equations (12) and (13) yields

$$\left.\begin{aligned} \vec{h}_{\ell,m,n} \cdot \vec{1}_x &= p_x + \frac{2\pi\ell}{a} \\ \vec{h}_{\ell,m,n} \cdot \vec{1}_y &= p_y + \frac{2\pi m}{a} \end{aligned}\right\} \tag{14}$$

where p_x and p_y are the x and y components of $\vec{p}_q$ (which are independent of q), and equation (9) then reads

$$\vec{h}_{\ell,m,n} \cdot \vec{1}_z = \pm \left[K^2 - \left(p_x + \frac{2\pi\ell}{a}\right)^2 - \left(p_y + \frac{2\pi m}{a}\right)^2\right]^{1/2} \tag{15}$$

The index, n, in the above equation may be dropped, and the wave function in the vacuum, equation (8), is written as

$$\Phi(\vec{r}) = \sum_{\ell,m} \left(\Phi^{-}_{\ell,m} \, e^{i\vec{h}^{-}_{\ell,m} \cdot \vec{r}} + \Phi^{+}_{\ell,m} \, e^{i\vec{h}^{+}_{\ell,m} \cdot \vec{r}} \right) \qquad z \gtrless 0 \qquad (16)$$

where $\vec{h}^{\pm}_{\ell,m}$ is a vector whose components are identical to those of $\vec{h}_{\ell,m,n}$ [equations (14) and (15)], with the exception that the superscript in $\vec{h}^{\pm}_{\ell,m}$ indicates the sign of its z-component. If there is only one incident electron beam, whose amplitude, $\Phi^{-}_{o,o}$, is equal to unity, equation (16) reduces to

$$\Phi(\vec{r}) = e^{i\vec{h}^{-}_{o,o} \cdot \vec{r}} + \sum_{\ell,m} \Phi_{\ell,m} \, e^{i\vec{h}^{+}_{\ell,m} \cdot \vec{r}} \qquad z \gtrless 0 \qquad (17)$$

where the first and second terms on the right hand side represent the incident and the diffracted electron beams, respectively.

It follows from equations (14) and (17) that the real parts of p_x and p_y are determined by the direction of incidence of the primary electron beam, whereas their imaginary parts must be zero, due to the boundary conditions at infinity. The z-components of the vectors $\vec{p}_q$, on the other hand, do not depend on the boundary conditions. Their real parts may, in principle, be chosen arbitrarily, within the interval $0 < \mathrm{Re}\left(p_{q_z}\right) < \frac{1}{a}$, and are usually assumed to be uniformly distributed throughout that interval. If however, the number of values of q, (i.e., the number of p_{q_z}'s) is small, a uniform distribution may not

be the optimum choice. Methods for finding the best possible values for the real parts of the p_{q_z}'s, as well as their imaginary parts, will be discussed below.

Introducing equation (17) into equations (10) and (11), and decomposing into a set of equations relating the coefficients of the various harmonics in x and y, leads to

$$\left.\begin{aligned} \sum_{n,q} \psi_{\ell,m,n,q} &= \Phi^{+}_{\ell,m} \qquad \ell \neq 0 \quad \text{or} \quad m \neq 0 \\ \sum_{n,q} \psi_{\ell,m,n,q} &= \Phi^{+}_{\ell,m} + 1 \qquad \ell = m = 0 \end{aligned}\right\} \tag{18}$$

$$\left.\begin{aligned} \sum_{n,q} \left(\vec{k}_{\ell,m,n,q} \cdot \vec{1}_z\right)\psi_{\ell,m,n,q} &= \left(\vec{h}^{+}_{\ell,m} \cdot \vec{1}_z\right)\Phi^{+}_{\ell,m} \\ &\qquad \ell \neq 0 \quad \text{or} \quad m \neq 0 \\ \sum_{n,q} \left(\vec{k}_{\ell,m,n,q} \cdot \vec{1}_z\right)\psi_{\ell,m,n,q} &= \left(\vec{h}^{+}_{\ell,m} \cdot \vec{1}_z\right)\left(\Phi^{+}_{\ell,m} - 1\right) \\ &\qquad \ell = m = 0 \end{aligned}\right\} \tag{19}$$

The quantity, $\Phi^{+}_{\ell,m}$, may be eliminated from equations (18) and (19), and we obtain

$$\left.\begin{aligned} &\sum_{n,q}\left(\left(\vec{k}_{\ell,m,n,q}-\vec{h}^{+}_{\ell,m}\right)\cdot\vec{1}_z\right)\psi_{\ell,m,n,q}=0 \\ &\qquad\qquad \ell\neq 0 \quad \text{or} \quad m\neq 0 \\ &\sum_{n,q}\left(\left(\vec{k}_{\ell,m,n,q}-\vec{h}^{+}_{\ell,m}\right)\cdot\vec{1}_z\right)\psi_{\ell,m,n,q}+2\left(\vec{h}^{+}_{\ell,m}\cdot\vec{1}_z\right)=0 \\ &\qquad\qquad \ell=m=0 \end{aligned}\right\} \tag{20}$$

or in matrix form,

$$\underset{\sim}{B}\underset{\sim}{\psi}=\underset{\sim}{\chi} \tag{21}$$

The compatibility equations (7) and the boundary condition equations (21) may be combined into one single equation,

$$\underset{\sim}{G}\underset{\sim}{\psi}=\underset{\sim}{H} \tag{22}$$

If the series representing the potential $W(\vec{r})$ and the electron wave function in the crystal and in vacuum are approximated by truncation, the matrix G has more rows than columns and, therefore, equation (22) has no exact solution. The best solution is found, according to the principle of least squares, by minimizing

$$S = (G\underset{\sim}{\psi} - \underset{\sim}{H}) \cdot D(G\underset{\sim}{\psi} - \underset{\sim}{H})^* \tag{23}$$

where D is a positive, real, diagonal matrix, containing suitable weighting coefficients, and * indicates complex conjugation. Since S is positive and quadratic in any of the unknowns, $\mathrm{Re}\left(\psi_{\ell,m,n,q}\right)$ and $\mathrm{Im}\left(\psi_{\ell,m,n,q}\right)$, the minimum is characterized by the conditions

$$\left.\begin{aligned} \frac{\partial S}{\partial \mathrm{Re}\left(\psi_{\ell,m,n,q}\right)} &= 0 \\ \frac{\partial S}{\partial \mathrm{Im}\left(\psi_{\ell,m,n,q}\right)} &= 0 \end{aligned}\right\} \quad \text{any } \ell,m,n,q \tag{24}$$

or, equivalently, in matrix form,

$$P\underset{\sim}{\psi} = \underset{\approx}{Q} \tag{25}$$

where P is now a square matrix. Equation (25) is solved, not by straightforward inversion of P, but by an iterative technique, which is not affected by round-off errors during the computation.

It should be noted that the elements of both P and $\underset{\approx}{Q}$ contain the components of the vectors $\vec{p}_q$. As was pointed out above, the x and y components of these vectors are independent of q and determined by the angles of incidence of the primary electron beam. If the z-components of the $\vec{p}_q$'s are treated as unknowns, they are determined by solving the equations

$$\left.\begin{aligned} \frac{\partial S}{\partial \mathrm{Re}\left(p_{q_z}\right)} &= 0 \\ \frac{\partial S}{\partial \mathrm{Im}\left(p_{q_z}\right)} &= 0 \end{aligned}\right\} \quad \text{any } q \tag{26}$$

simultaneously with equation (25). If we choose to represent the wave function in the crystal by a single Bloch wave, i.e., if we consider only one q, we find that $\mathrm{Re}\left(p_q\right)$ is very nearly equal to $-\left(K^2 + \mathrm{Re}\left(w_{o,o,o}\right)\right)^{1/2}$, whereas $\mathrm{Im}\left(p_{q_z}\right)$ approaches $-\mathrm{Im}\left(w_{o,o,o}\right)/2\left(K^2 + \mathrm{Re}\left(w_{o,o,o}\right)\right)^{1/2}$ for large values of $\mathrm{Im}\left(w_{o,o,o}\right)$. Obviously, once the vector $\underset{\sim}{\psi}$ is known, the intensities of the diffracted beams, i.e., $\left|\Phi^{+}_{\ell,m}\right|^2$, are computed readily from equations (18) and (19).

III. BEAM INTENSITY CALCULATIONS

Using the theory outlined above, calculations were performed under the following conditions:

(1) A primary electron beam of unit intensity is incident normally on the (100) surface of a fcc lattice, with lattice constant, a = 4.04 Å (aluminum).

(2) The crystal lattice is represented by a complex potential. The shape of its real part, i.e., the relative magnitude of the expansion coefficients, $w_{\ell,m,n}$ [equation (1)], is obtained by Fourier-analyzing the "self consistent"

aluminum potential given in reference 8. The expansion includes all terms for which $\ell^2 + m^2 + n^2 \leq 4$, and the imaginary part of the potential is assumed independent of position and electron energy.

(3) The crystal surface, where the potential abruptly drops to zero, lies half-way between two layers of atoms.

(4) The wave function in the crystal is approximated by a single Bloch wave [only one $\vec{p}_q$ in equation (5)] whose expansion is truncated such that $\ell^2 + m^2 + n^2 \leq 34$.

Figure 1. illustrates the dependence of the beam intensity vs energy curves on the assumed inner potential $\left(\mathrm{Re}\left(w_{o,o,o}\right)\right)$. Decreasing the inner potential by 2.5 volts translates the curves to a commensurate, higher energy.

Figure 2. shows the dependence of the beam intensities on the magnitude of the oscillatory part of the potential, i.e., on the elastic scattering cross section. The latter quantity is varied by introducing a scaling factor that multiplies all coefficients, $w_{\ell,m,n}$, except $w_{o,o,o}$. For small cross sections, only the ordinary Bragg peaks are present. As the cross section is made larger, secondary Bragg peaks and resonance phenomena, due to multiple scattering effects, appear.

Figure 3. demonstrates the dependence of the intensity curves on the magnitude of the imaginary potential, i.e., on the inelastic scattering cross section. As the imaginary potential decreases, the amount of "structure" (peak-to-valley ratios) increases considerably. This behavior is to be expected. A decrease in the inelastic scattering enhances the penetration of the primary beam and, therefore, enhances all three-dimensional effects. Clearly, the very existence of Bragg peaks or structure is a three-dimensional effect par excellence. The disappearance of the secondary Bragg peaks for large values of the imaginary potential, as seen in Figure 3, indicates that these peaks may be attributed to multiple scattering events involving atoms in different layers, rather than atoms in a single layer.

IV. COMPARISON WITH EXPERIMENT

Beam intensity measurements on the (100) surface of aluminum single crystals are being performed by Dr. S. M. Bedair at our laboratory. Figure 4 compares his measurements[7] with a typical set of our theoretical curves. All three experimental curves are normalized to the same primary electron beam current. Intensity ratios between different beams are, therefore, represented correctly.

When considering this comparison between theory and experiment (Figure 4), the following points should be borne in mind:

(1) No attempt has been made to optimize the parameters of the potential, i.e., the expansion coefficients $w_{\ell,m,n}$.

(2) The imaginary part of the potential has been assumed constant, whereas it should vary with electron energy in order to represent the known variation of inelastic scattering cross sections with energy.

(3) The theoretical results reported here are based on a single Bloch function representation. It remains to be investigated whether this is a good approximation or there are cases where a more rigorous multi-Bloch function treatment must be used.

A thorough parameter optimization, along the lines indicated above, might improve the agreement between theory and experiment considerably. This would, however, represent a very large investment in computer time.

V. CONCLUSIONS

We have shown that an extended Bethe theory (Section II of this paper) may be applied successfully to the computation of LEED intensities. The results are in reasonable agreement with measured[7] beam intensities (Figure 4), although we have used a single Bloch function approximation in order to avoid an excessively lengthy calculation and

there are at least two limitations inherent in our model that have to be seriously questioned.[1] These are the uses of an incident plane wave and the assumed perfect periodicity with abrupt cutoff at the crystal surface.

References

[1]E. G. McRae, J. Chem. Phys. *45*, 3258 (1966).

[2]K. Hirabayashi and Y. Takeishi, Surface Sci. *4*, 150 (1966).

[3]D. S. Boudreaux and V. Heine, Surface Sci. *8*, 426 (1967).

[4]F. Hofmann and Harold P. Smith, Jr., Phys. Rev. Letters *19*, 1472 (1967).

[5]P. M. Marcus and D. W. Jepsen, Bull. Am. Phys. Soc., Series II, *13*, 367 (1968).

[6]H. Bethe, Ann. Physik *87*, 55 (1928).

[7]S. M. Bedair, private communication.

[8]E. C. Snow, Phys. Rev. *158*, 683 (1967).

PARTICIPATING PERSONNEL

Professor Harold P. Smith, Jr.	— Principal Investigator
Ferdinand Hofmann	— Assistant Research Engineer
Yeong-du Song	— Research Assistant

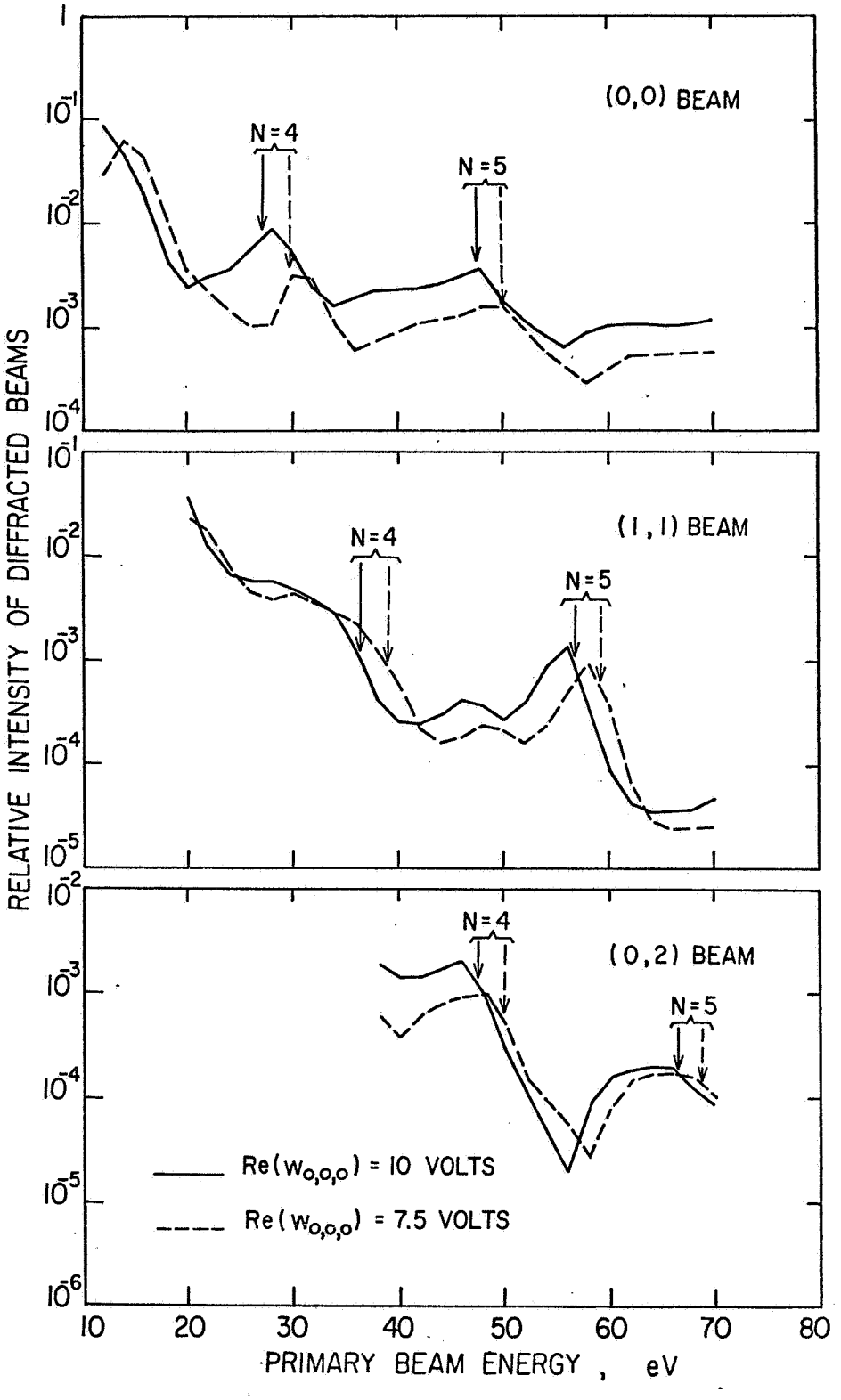

FIGURE 1. Calculated beam intensities vs energy, showing the dependence on the inner potential. Conditions: imaginary part of potential $Im(w_{o,o,o})$ = 2.5 volts and elastic scattering cross section scaling factor = 1.0. The arrows indicate Bragg relections of order N where the inner potential correction has been included. Beams with mixed indices are absent due to symmetry of the fcc lattice.

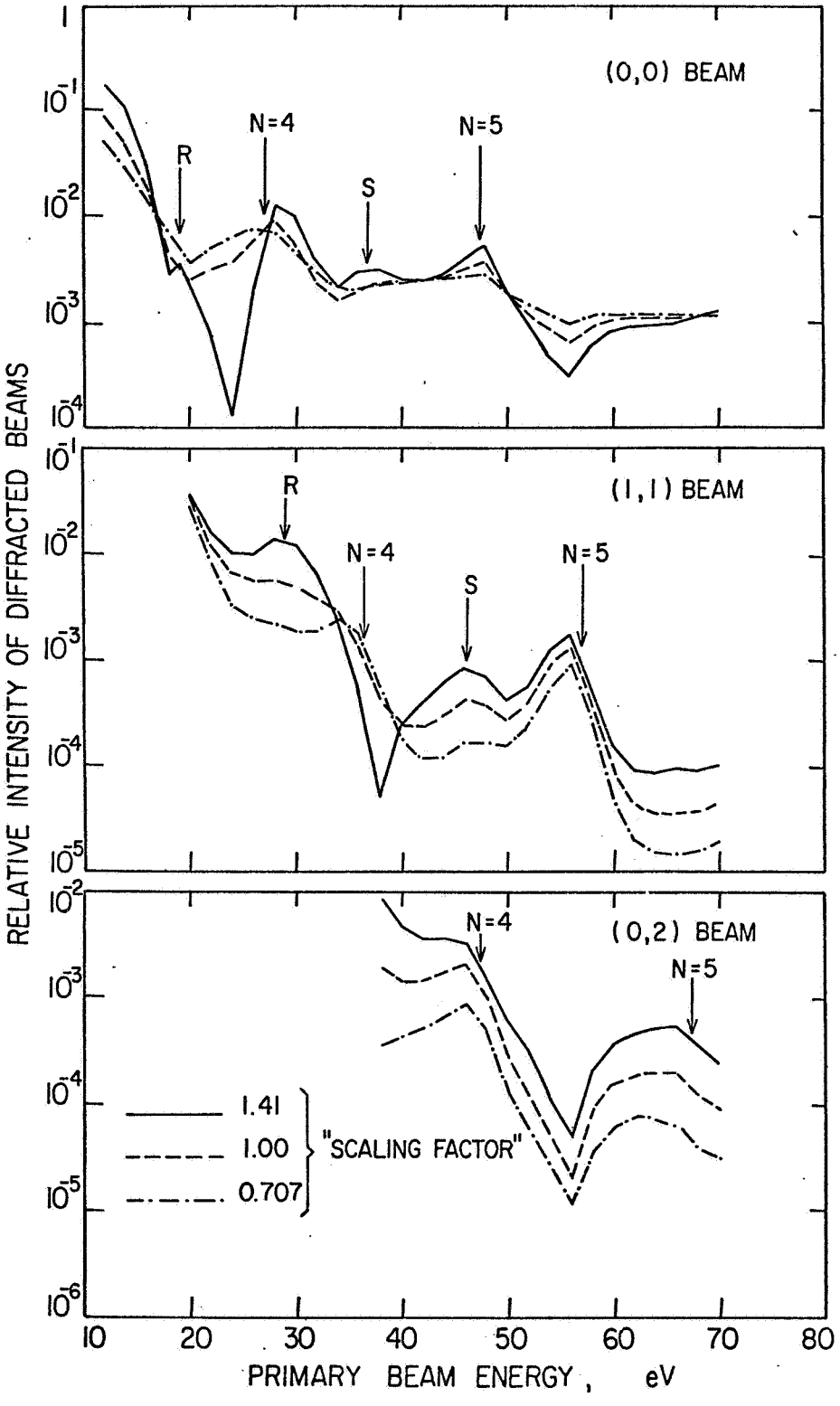

FIGURE 2. Calculated beam intensities vs energy, showing the dependence on the elastic scattering cross section (scaling factor). Conditions: inner potential $Re(W_{o,o,o}) = 10$ volts, imaginary part of potential $Im(w_{o,o,o}) = 2.5$ volts. The order of the Bragg reflections is indicated by N. The letters S and R designate secondary Bragg and resonance peaks.

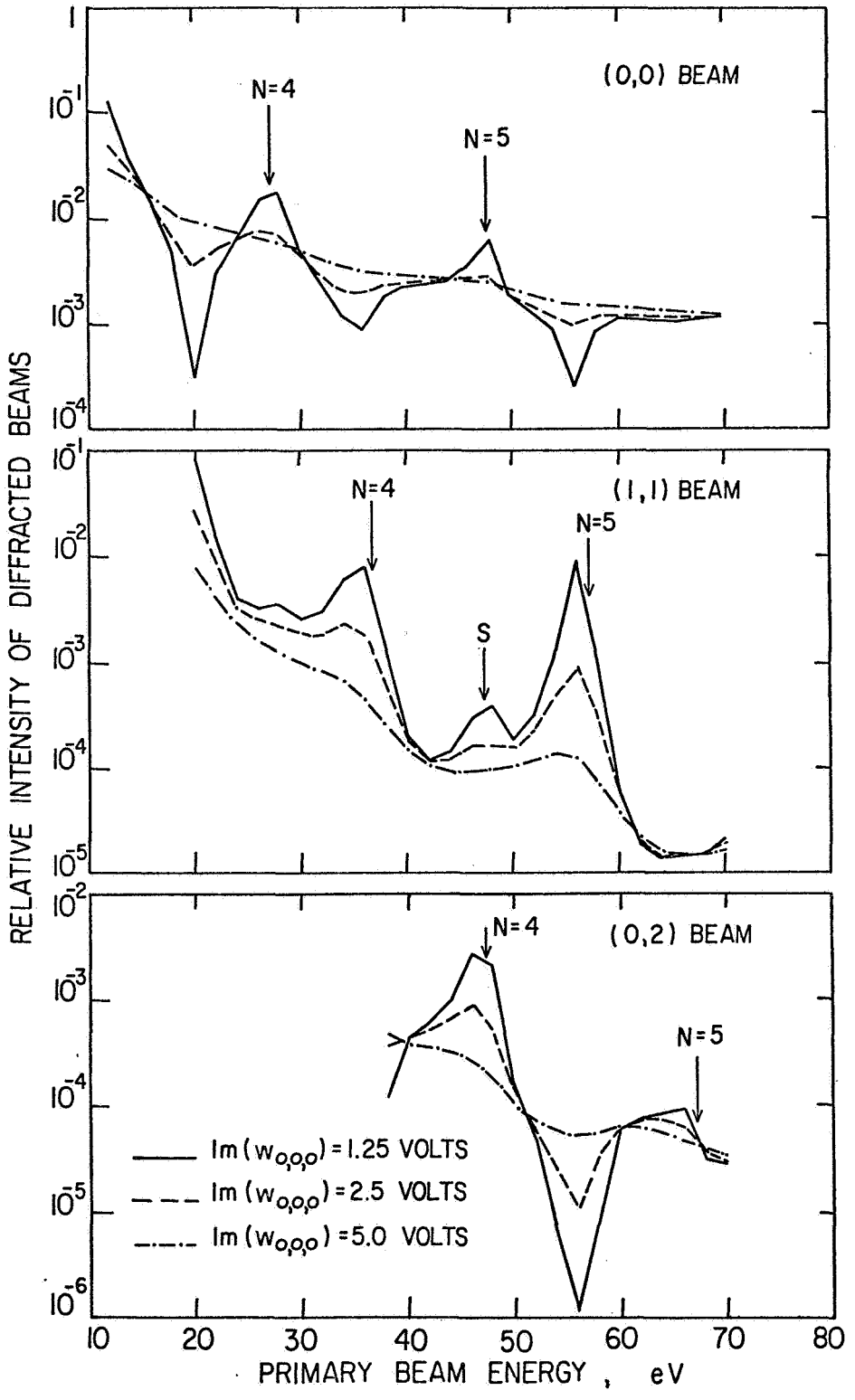

FIGURE 3. Calculated beam intensities vs energy, showing the dependence on the imaginary potential. Conditions: inner potential $Re(w_{0,0,0})$ = 10 volts, scaling factor = 0.707. The letter N indicates the order of the Bragg reflections, and S denotes a secondary Bragg peak.

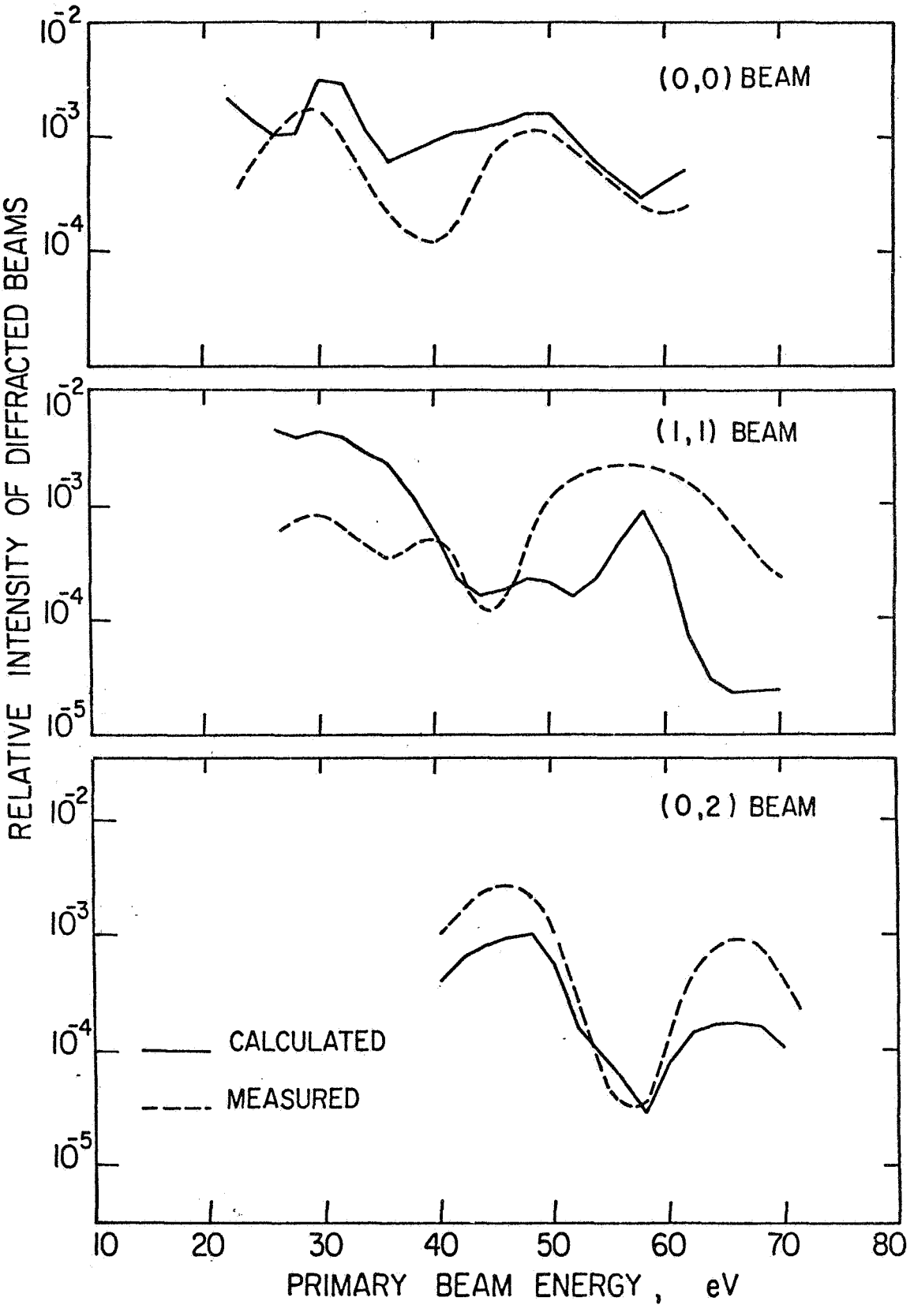

FIGURE 4. Comparison between measured[7] and calculated beam intensities vs energy. Theoretical conditions are as noted in Figure 1 and experimental conditions are aluminum (100) surface, normal incidence.